Dissociative recombination of H_2^+: Product state information and very large cross sections of vibrationally excited H_2^+

Wim J. van der Zande,[2] Jacek Semaniak,[1] Veysel Zengin,[1,*] Göran Sundström,[1,*] Stefan Rosén,[1] Christian Strömholm,[1] Sheldon Datz,[3] Håkan Danared,[4] and Mats Larsson[1]

[1]*Physics Department I, The Royal Institute of Technology, S-100 44 Stockholm, Sweden*

[2]*FOM-Institute for Atomic and Molecular Physics, Kruislaan 407, 1098 SJ Amsterdam, The Netherlands*

[3]*Physics Division, Oak Ridge National Laboratory, Oak Ridge, Tennessee 37831-6377*

[4]*Manne Siegbahn Laboratory at Stockholm University, S-104 05 Stockholm, Sweden*

(Received 1 February 1996)

We report experiments on dissociative recombination (DR) of HD^+ and H_2^+. Product state information has been obtained over a wide range of electron energies with a position sensitive detector consisting of a graded absorber in combination with a surface-barrier detector. At low electron energies (<3 eV) hydrogen atoms are formed preferentially in highly excited states ($n>2$); at high electron energies (>12 eV) both hydrogen fragments are excited. The dissociative recombination rate of H_2^+ has been measured also as a function of storage time in the energy range of 0 eV to 20 eV. We show that the H_2^+ beam is still vibrationally excited after 20 s at our experimental conditions. The H_2^+ ions relax vibrationally through interaction with electrons in the electron cooler. Vibrationally excited levels ($v \geq 5$) have DR rates that exceed the DR rate of the lower vibrational levels by two orders of magnitude. The latter observation has important consequences for the interpretation of previous DR experiments on H_2^+. [S1050-2947(96)07012-6]

PACS number(s): 34.80.Gs

I. INTRODUCTION

The interest in dissociative recombination (DR) stems not only from its practical importance but also from its, at first sight, appealing simplicity: one electron recombines with (in this case) the simplest of molecules H_2^+. The practical aspects refer to laboratory [1], atmospheric [2], and astrophysical plasmas [3,4]. DR is often a quantitatively important process in these circumstances. The magnitude of the DR cross section of H_3^+ is even of paramount importance for the interpretation of cosmic abundance measurements [5–7]. Although DR seems to be a simple process, both the theory and experiment provide big challenges. Theoretical progress [8,9] has often been inspired by observations of sizable cross sections where theory had predicted vanishing small cross sections. DR is found to be especially efficient in systems where doubly excited neutral curves cross the ground-state ionic curve (plus zero-energy electron), as in the case of H_2^+ [10]. DR consists of three parts: (i) the electron capture process; (ii) the competition between dissociation and autoionization, ''survival''; and (iii) the molecular dissociation, a ''half collision.'' The cross section is determined by (i) and (ii). The distribution over the product states is governed by (iii). Experiments using various techniques (flowing afterglow's [11,12], merged-beams techniques [13,14], and ion-storage rings [15–19]) have produced ambiguous results. Ion-storage rings have distinct advantages. The lifetime of the ions and the electron-cooler technology have resulted in a significantly improved signal to noise and a high electron collision–energy resolution (10 meV) [20]. In CRYRING (Cryogenic Ion Source Ring) absolute cross sections have now been determined for H_2^+ (and its isotopomers) [18,19,21], HeH^+ [22,23] and, H_3^+ (and isotopomers) [17,24–26] over a wide electron energy range. Product state information or branching ratios have only recently been the aim of experiments. Datz *et al.* [26] introduced a ''translucent'' perforated foil to study the fragmentation behavior in the case of H_3 and its isotopomers [25]; H+H+H could be distinguished from $H+H_2$, and HD+H from $D+H_2$ and H+H+D. The first report on product state distributions stems from TARN II (Test Accumulation Ring for the Numatron Accelerator Facility) experiments on HeH^+. The channel forming excited-state hydrogen atoms was observed to dominate [27]. Very recently Zajfman *et al.* reported very detailed product state and angular distributions using HD^+ [28]. This isotopomer of H_2 was chosen because the storage time allows complete radiative cooling of all vibrationally excited states.

We report product state distributions of H_2^+ at various electron collision energies using a simple position-sensitive detector in the form of a graded absorber built from a wedge shaped Cu foil. Total DR rates of H_2^+ are observed to decrease as function of storage time. It is argued that the high vibrational levels have very high DR rates. We will present the experimental technique, the principle of our graded absorber detector [29], our experimental results and we will discuss their consequences.

II. EXPERIMENT

The experiments are performed in CRYRING, an ion storage ring device at the Manne Siegbahn Laboratory in Stockholm [20,30]. A schematic diagram of CRYRING is shown in Fig. 1. The H_2^+ or HD^+ ions are produced in the electron-impact ion source MINIS, then extracted and mass

*Present address: Department of Chemistry, University of California, San Diego, CA.

**Present address: Ericsson Telecom AB, S-126 25 Stockholm, Sweden.

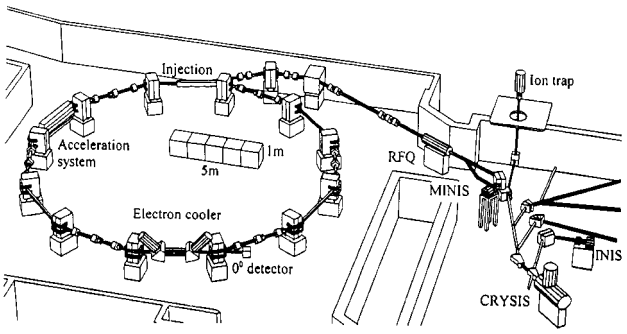

FIG. 1. The CRYRING facility at the Manne Siegbahn Laboratory at Stockholm University. The circumference of the ring is 52 m. Dissociative recombination takes place in the electron-cooler section (length 0.8 m) imbedded in a straight section of 1.7 m. The neutral products of dissociative recombination are detected in the 0° detector arm.

selected. Before injection the ions are accelerated to 300 keV/amu. In the ring the ions are further accelerated to various energies between 4 MeV/amu and 5.4 MeV/amu. The ion storage ring contains an electron-cooler section meant for phase-space cooling. This is also the place where dissociative recombination takes place. As a consequence of the phase-space cooling, a strong reduction of the beam size to less than 1 mm takes place in about 2 sec (at 50 mA electron current). After a further (variable) delay time a DR measurement is started by changing the energy of the electrons from the cooling energy (E_{cool}) to the measuring energy (E_{meas}). The relation between the measuring energy and the collision energy in the center-of-mass frame (E_{rel}) is given by

$$E_{\mathrm{rel}}=(\sqrt{E_{\mathrm{meas}}}-\sqrt{E_{\mathrm{cool}}})^2. \tag{1}$$

In order to avoid heating of the ion beam, the electron energy is changed only during short, typical 100 ms, intervals, especially for small values of E_{rel}. A DR event leads to the formation of two neutral atoms which are detected in coincidence in the so-called 0° arm of the storage ring. The lifetime of the ion beam is affected by collisions with residual gas. At MeV energies, these collisions result in the production of at most one neutral fragment. Its translational energy is half of that of two fragments. Thus background and DR signal are easily distinguished using the surface-barrier detector (SBD).

$$H_2^+(v',J')+e^-(E_{\mathrm{rel}})\rightarrow H(1s)+H(nl) +E_{\mathrm{KE}}(v',J',n,E_{\mathrm{rel}}). \tag{2}$$

Reaction (2) shows the relation between the internal energy of an H_2^+ ion, the internal energy of fragment atoms, the electron energy, which is an experimental parameter, and the kinetic energy E_{KE} released in DR process. The rovibrational distribution of an H_2^+ beam from an electron-impact source has been well documented, but the effect of the long storage times on the distributions is not known. For each rovibrational level (v',J'), the principal quantum number (n) of the hydrogen fragment, the electron energy (E_{rel}) and the E_{KE} are directly related. For H_2^+ $(v'=0, J'=0)$, the released

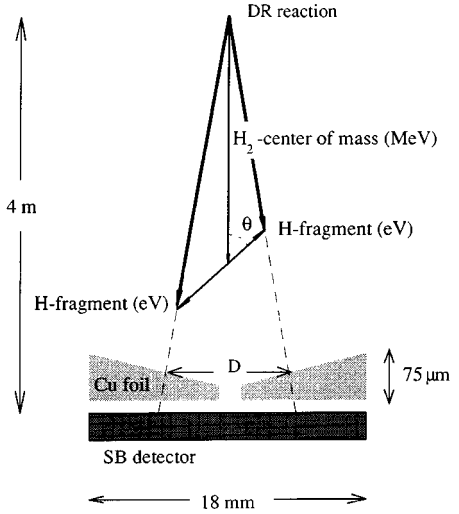

FIG. 2. Schematic diagram of the position sensitive detector consisting of the surface-barrier detector (SBD) and a cylindrically symmetric wedged shaped Cu foil. The recoil velocity of the H fragments due to the dissociative recombination process is reflected in the distance D. The foil acts as a graded absorber, translating D into energy loss of the fragments.

kinetic energy equals $E_{\mathrm{KE}}=E_{\mathrm{rel}}+13.6\ n^2-2.65$ (eV). The value of 2.65 eV is the binding energy (D_0) value of the H_2^+ electronic ground state.

The technique with the graded absorber is based on the recoil velocity of the fragments released in the dissociation process. To detect the recoil of the fragments a position-sensitive detector (diameter 18 mm) is mounted 4 m behind the interaction region. The detector consists of a cylindrical-symmetric, wedge shaped copper foil followed by a surface-barrier detector (SBD), see Fig. 2. The foil acts as a graded absorber. It has a small hole (0.45 mm diameter) in the middle for alignment purposes, and its thickness increases monotonic from 15 to 60 μm. The graded absorber is produced by mechanical means. Atoms lose kinetic energy upon transiting the foil. The energy loss depends on the distance from the beam axis (see Fig. 2). Thus an increase in the projected distance D between DR fragments results in an increase in the total energy loss of both fragments. Being measured simultaneously, the sum of their kinetic energies is detected. The thickness of the foil is chosen so that the maximum energy loss is less than 50%. Thus, DR events are detected at laboratory energies, $E_{\mathrm{lab}}>0.5\times E_0$, where E_{lab} is recorded by the SBD and E_0 is the full beam energy; background counts are observed at $E_{\mathrm{lab}}<0.5\times E_0$.

The measurement principle is only reliable with an ion beam that is significantly smaller than the projected distance D and that is properly centered. In the case of the H_2^+ data the diameter of the beam can be expected to be about 800 μm full width at half maximum (FWHM) as was determined using a deuterium ion beam. Further resolution limiting factors are energy straggling of the fragments and thickness irregularities of the mechanically machined Cu foil. Since the detector signal is a measure for the projected distance D, different angles of dissociation (θ) result in a distribution in D. Also, D is proportional to the distance from the collision center to the detector. The finite length of the electron cooler

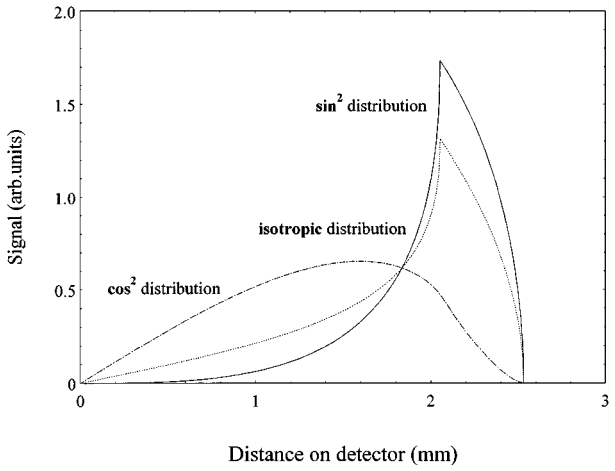

FIG. 3. Typical D distributions involving a single kinetic-energy release value and different possible angular distributions. The shape of the tails at small distance reflects the angular distribution, the ''shoulder'' at large distances is due to the finite length of the interaction region, the electron cooler section.

of approx. 80 cm results in a 20% spread in D. Figure 3 shows three examples of D distributions involving one single kinetic-energy value of the fragments. These distributions take the finite interaction length and three possible fragment-angular distributions (isotropic, $\cos^2$, $\sin^2$) into account. Fortunately, still distinct peaklike features result. Figure 4 shows simulations that include the foil parameters and the finite beam size. E_{lab} spectra are shown using E_{KE} values of 0.75 eV $[H_2^+(v'=0)+e^-(0\ \mathrm{eV})\rightarrow H(1s)+H(2s)]$ and 2.0 eV $[H_2^+(v'=5)+e^-(0\ \mathrm{eV})\rightarrow H(1s)+H(2s)]$. An isotropic dissociation has been assumed. The small peak at 10.8 MeV is due to two fragments through the 0.45 mm hole. The peak at 10.2 MeV reflects events with one hydrogen atom through the hole. The resolving power is clearly insufficient to distinguish individual vibrational levels (0.25 eV spacing) but sufficient to observe effects associated with different $H(n,l)$

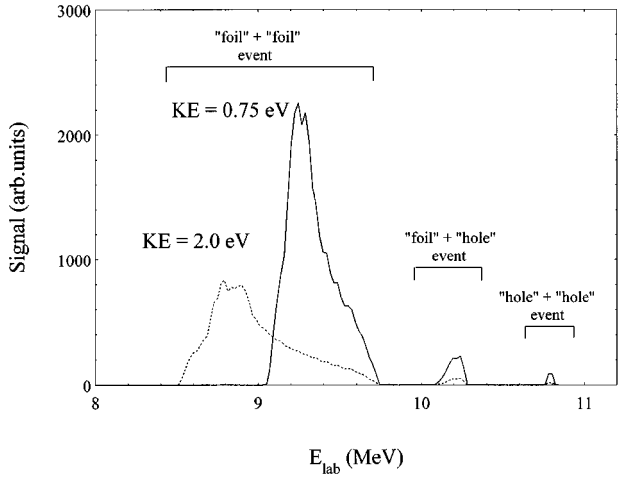

FIG. 4. Simulations of spectra from the SBD+graded absorber using values for kinetic-energy values of $E_{\mathrm{KE}}=0.75$ eV and 2.0 eV using the dimensions of the ion beam and foil. An isotropic distribution is assumed in these simulations.

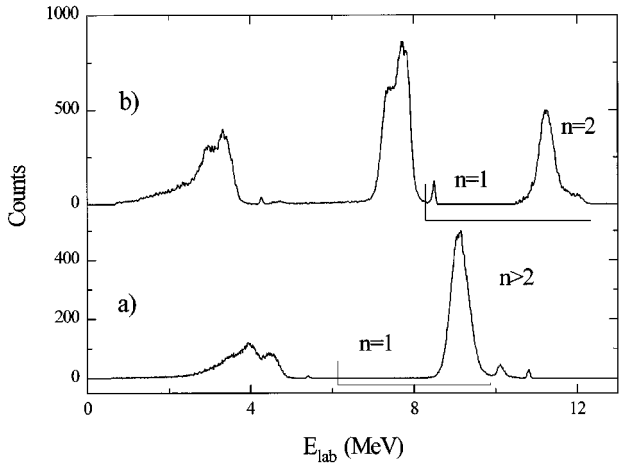

FIG. 5. E_{KE}-spectra measured at $E_{\mathrm{rel}}=0$ eV for (a) 10.8 MeV H_2^+ after a storage time of $t=20$ s and (b) 12 MeV HD^+. The spectra show counts as function of the total energy of both fragments after the graded absorber (E_{lab}). The high-energy structures above (a) 5.4 MeV and (b) 8.2 MeV reflect DR. The low-energy structures are collisional background and are a measure of the ion current. The thin lines, labeled $n=1$ indicate the range in E_{lab} for the formation of $H(n=1)+H/D(n=1)$ products. The labels, $n=2$, indicate that the peak positions agree with $H(n=2)+H(n=1)$ products.

dissociation limits (e.g., the 1.89 eV spacing between $n=2$ and $n=3$). Spectra, such as Fig. 4, show the laboratory energy (E_{lab}) of the two fragments after the graded absorber and are called E_{KE} spectra. We stress, however, that one value of the kinetic energy gives a distribution in an E_{KE} spectrum.

Experiments have been performed with the graded absorber at various electron energies (E_{rel}) from 0 eV to 18 eV and after different storage times. Experiments on HD^+ are performed to differentiate intramolecular cooling from other time-dependent effects in the ion storage ring. Spectra have been collected using the graded absorber (for E_{KE} spectra) and with a standard ''bare'' SBD (for DR-rate determinations only). The relative DR rate is defined as the ratio between the ''DR-signal'' channel (two neutral fragments) and the ''background'' channel (one neutral fragment). The background channel is a measure for the number of ions in the ring [31–33]. At large electron collision energies the background channel increases due to dissociative excitation. With the use of a multichannel scaler (set to background) and a multichannel analyzer, these changes are recorded and the DR rates are corrected. The DR rate is a product of $\langle v\sigma\rangle$ (the specific rate of DR process, with v the relative collision velocity, the brackets represent the averaging over the velocities), and n_e (the electron density, proportional to the electron current). In principle, absolute cross sections (σ) can be extracted [22,32,33].

III. RESULTS

A. Product state distributions

Figure 5 shows total E_{KE} spectra measured by means of the graded absorber at $E_{\mathrm{rel}}=0$ eV taken at a beam energy of 5.4 and 4.5 MeV/amu for H_2^+ and HD^+ ions, respectively.

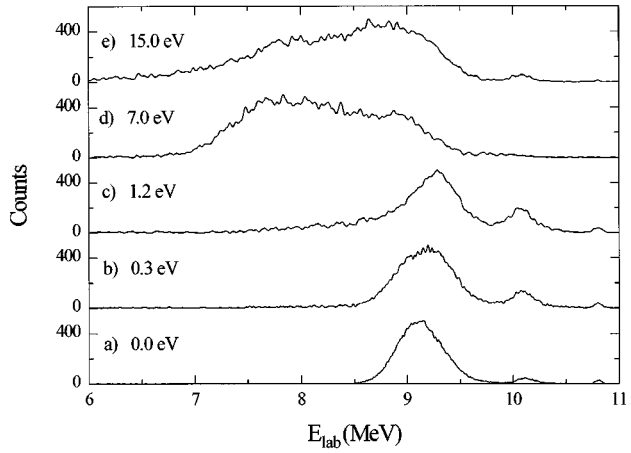

FIG. 6. E_{KE}-spectra from the $e^-+H_2^+$ dissociative recombination process at electron collision energies (E_{rel}) of (a) 0.0 eV, (b) 0.3 eV, (c) 1.2 eV, (d) 7.0 eV, and (e) 15.0 eV.

The spectra were measured after a storage time of 20 s. Background is found below 5.4 MeV (curve *a*) and 8.2 MeV (curve *b*). The relevant part of the spectra is at $E_{lab} \geqslant 5.4$ MeV and $E_{lab} \geqslant 8.5$ MeV for the H_2^+ and HD^+ experiment, respectively. As in Fig. 4, small features are seen at high energy reflecting the hole in the foil. Figure 6 displays a few spectra taken at different values of E_{rel}. Results for HD^+ are shown in Fig. 7. Before discussing these results, Fig. 8 is introduced.

Figure 8 (adapted from Ref. [10]) shows the relevant potential curves for molecular hydrogen [10,34]. The two lowest dissociation limits ($H(n=1)+H(n=1)$ and $H(n=2)+H(n=1)$) are energetically accessible for $E_{rel}=0$ eV and $H_2^+(v^+=0)$; the E_{KE} values are $E_{KE}=0.75$ eV for $H(n=1)+H(n=2)$ and $E_{KE}=10.95$ eV for $H(n=1)+H(n=1)$. At $E_{rel}=1.14$ eV the total energy suffices for the formation of $H(n=3)$ fragments. The cross section of DR via the doubly excited $^1\Sigma_g^+$ repulsive state has a maximum around $E_{rel}=4$ eV [18]. At higher collision energies the cross section increases due to the other Q_1 states with $^1\Sigma_u^+$, $^1\Pi_g$, $^3\Sigma_u^+$, and

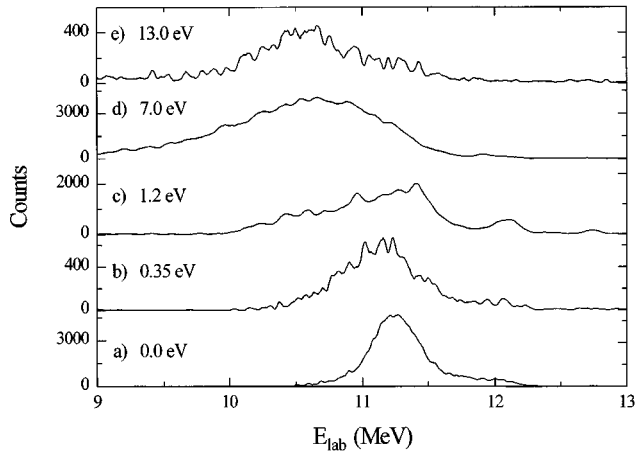

FIG. 7. E_{KE}-spectra from the e^-+HD^+ dissociative recombination process at electron collision energies (E_{rel}) of (a) 0 eV, (b) 0.35 eV, (c) 1.2 eV, (d) 7.0 eV, and (e) 13.0 eV.

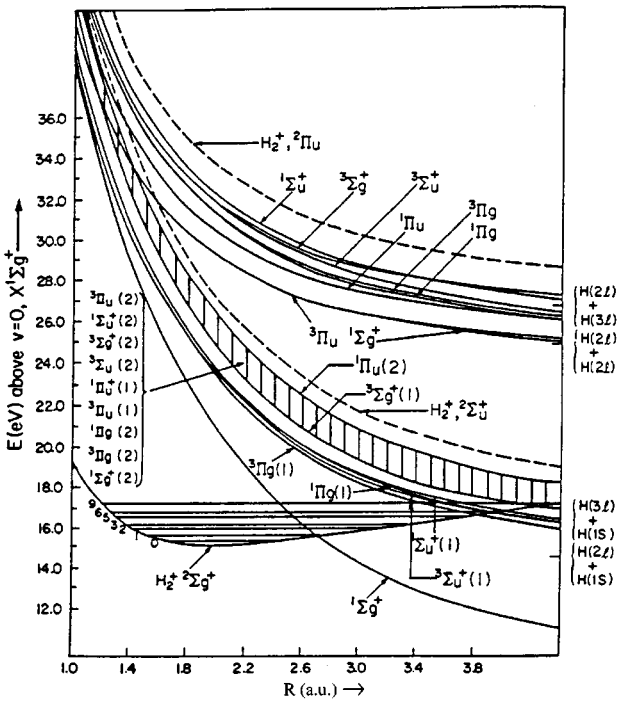

FIG. 8. Potential-energy curves (in units of eV) as function of internuclear separation in a.u. for H_2 and H_2^+. The curves relevant to the dissociative recombination process have been shown. The vibrational levels in the H_2^+ ground state are indicated. The curves labeled H_2^+ should be read as potential energy of H_2^+ with a 0 eV electron. The other curves pertain to neutral doubly excited H_2 (taken from Ref. [10]).

$^3\Pi_g$ symmetry. We note that for higher-vibrational levels ($v \geqslant 5$) a significant overlap already exists with these higher Q_1 states at zero electron energy. At higher electron energies ($E_{rel}>12$ eV) the doubly excited repulsive (Q_2) states may be formed that correlate with two excited atoms. The nomenclature is taken from Guberman [10].

Now, the observed spectra of Figs. 6, 7 will be discussed in more detail. The range in E_{lab} from 6 to 11 MeV (for H_2^+) and from 9 to 13 MeV (for HD^+) is shown for the different spectra. With respect to the simulation (Fig. 4), the shape of the peak registered for H_2^+ ions is broader and more symmetric. An important observation is the absence of dissociation to $H(n=1)+H(n=1)$ for all E_{rel} values. The changes found in the H_2^+ spectra for electron energies, E_{rel}, between 0.0 eV and 0.5 eV are surprising. The signal intensity around 10.2 MeV increases (more dissociation with one fragment through the hole). Also, the maximum of the peak around 9.2 MeV shifts to higher, E_{lab}, energy (smaller energy loss). We conclude that the E_{KE} values *decrease*. Based on available energy, we conclude that higher excited ($v^+ \geqslant 4$) levels are present in the beam, which preferentially yield $H(n=3)$ fragments. In going from $E_{rel}=0.1$ eV to 1.2 eV the maxima of the distributions continue to shift to higher E_{lab} values. The E_{KE} values still decrease. The smallest E_{KE} values were observed at an electron energy of 1.2 eV [Fig. 6(c)]. At this collision energy all vibrational levels may dissociate to $H(n=3)$ fragments. At a collision energy above 1.2 eV the position of the peaks shifts back. We conclude that a strong

propensity exists to produce H($n=3$) final states as soon as it is energetically allowed.

An HD^+ beam consists of $v^+=0$ ions due to the allowed radiative decay of higher vibrational levels. Here an increase in E_{rel} results in a shift to lower E_{lab} values [an increase in E_{KE}, Fig. 7(a), 7(b)]. The broad features in the E_{KE} spectra [Fig. 7(b), 7(c)] do not imply the presence of vibrationally excited species. The graded-foil technique is less accurate for a heteronuclear species. Moreover, in the HD^+ experiment the size and shape of the beam has not been determined. Simulations of spectra indicate that the HD^+ beam was significantly larger than the H_2^+ beam. Therefore, we restrict ourselves to qualitative changes of the HD spectra. At an electron energy of 1.2 eV, the peak has broadened indicating that [Fig. 7(c)] H/D($n=3$) is produced as well as H/D($n=2$).

For both H_2^+ and HD^+ [Fig. 6(d), 7(d)], an increase in E_{rel} results in an increase of E_{KE} until $E_{rel}=12$ eV, above which a sudden shift is observed towards high E_{lab} and thus a smaller E_{KE} value. The spectra at $E_{rel}=15$ eV [Fig. 6(e), H_2^+] and $E_{rel}=13$ eV [Fig. 7(e), HD^+] can only be understood as due to two excited atomic fragments.

The important conclusions are (i) no DR is observed to ground-state hydrogen atoms; (ii) H_2^+ has a propensity to maximize the internal energy in the hydrogen fragments at small electron energies; (iii) at high energies two excited fragments are observed; and (iv) the H_2^+ ion beam is vibrationally hot after 20 s of storage time. The first three conclusions are in agreement with the results on HD^+ as reported recently by Zajfman and co-workers [28].

B. Vibrational cooling dynamics in the storage ring

The dissociative recombination rate strongly depends on the vibrational state of the ion. Therefore, knowledge of the H_2^+ ion-beam composition is required for absolute measurements. The long storage times are not expected to give vibrational cooling. For H_2^+ and HD^+, Amitay, Zajfman, and Forck [35] have reported relative rates for different storage times less than 1 s. They showed a fast decrease of the observed HD^+ DR rate in 0.2 s, attributed to vibrational relaxation by infrared emission. In H_2^+, radiative decay is forbidden and extremely slow. In a series of experiments we have followed the DR rate (for 0 eV$\leqslant E_{rel}\leqslant$20 eV) and the product state distribution (for $E_{rel}=0$ eV, at the maximum DR rate) as a function of storage time (up to 240 s in some cases).

Figure 9 shows measured DR rates as a function of E_{rel} for HD^+ and for H_2^+ for different storage times. Each of the curves shows the rapid decrease at $E_{rel}>0$ eV in accord with Wigner's threshold law. Apart from curve (d) all show a clear maximum in the cross section around $E_{rel}=6-9$ eV. We find (i) that the DR rate at low energy strongly decreases with increasing storage time; and (ii) that the high-energy ''resonance'' structure becomes more pronounced and shifts to higher energy (in the direction of the asymptotic position of the resonance observed for HD^+). Both these effects suggest a change in the H_2^+ beam population. The mechanism for these vibrational changes is yet unknown.

Figure 10 shows the DR rates for H_2^+ and HD^+ as a function of storage time (measured at $E_{rel}=0$ eV). The DR rate for H_2^+ strongly decreases between $t=4$ s and $t=10$ s,

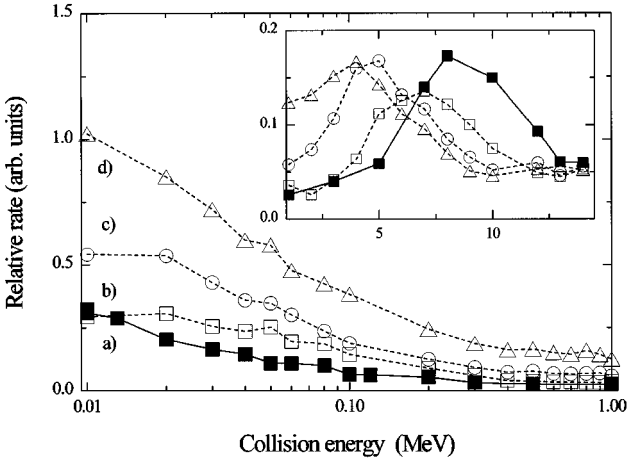

FIG. 9. Dissociative recombination rates for HD^+ [curve (a), solid squares] and H_2^+ as function of collision energy E_{rel} in units of eV for selected storage times of (b) 54 s-□; (c) 20 s-○; and (d) 5 s-△. The inset shows the high electron energy E_{rel} part of the distributions.

followed by a slower decrease. The control experiment with HD^+ [Fig. 10(b)] shows that after about 3 s (the estimated phase-space cooling time) the DR rate for HD^+ is constant. Possible mechanisms for the vibrational relaxation of H_2^+ are intramolecular decay (by radiative cooling), collisions with rest gas, (pre)dissociation by the motional fields in the bending magnets, or collisions with the cooler electrons. The latter effect can be simply isolated. The solid squares show the result of a delayed onset of the electron-cooler beam (30 s after ion injection). The curves are the same. Also the E_{KE} spectra (Fig. 11) did not change by the 30 s storage of ions without cooler electrons. It is concluded that the changes in DR rate are caused by collisions with electrons at $E_{rel}=0$ eV. Moreover, we conclude from Fig. 10 that dissociative collisions with rest gas do not change the vibrational population. Hence, the background channel can be used as a monitor of the ion-beam intensity.

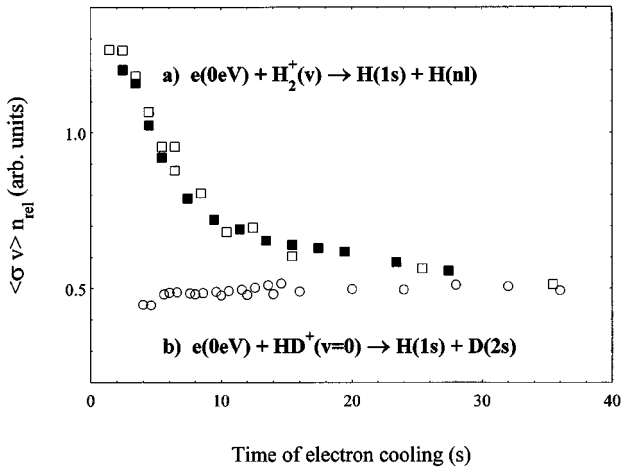

FIG. 10. The relative DR rates for HD^+ (○) and H_2^+ ( ) at $E_{rel}=0$ eV as a function of storage time. The data signed by solid squares show the rates measured with a 30 s delay of the electron cooling.

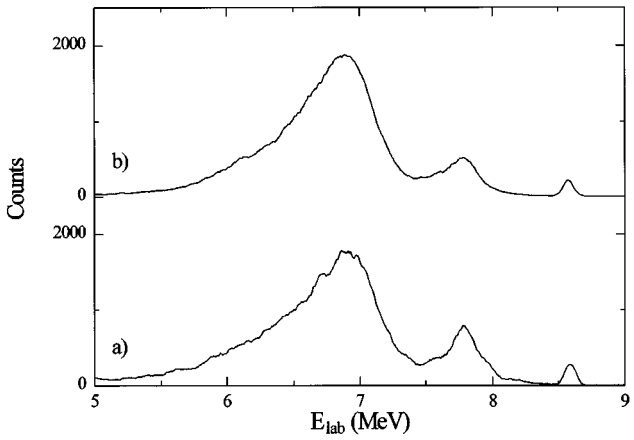

FIG. 11. E_{KE} spectra of DR of H_2^+ at $E_{rel}=0$ eV measured after 3.5 s electron-cooling time with a 0 s [curve (a)] and a 30 s delay [curve (b)] for the onset of electron cooling.

Electron-ion collisions can change the ion-beam rovibrational population through the dissociative recombination process and through superelastic collisions (SEC) [36] (see reaction 3)

$$H_2^+(v',J')+e^-(E_{rel}=0\ \text{eV})\rightarrow H_2^+(v'-1,J')+e^-(E_{rel}>0\ \text{eV}). \qquad (3)$$

In DR, ions disappear while in SE collisions the number of ions is unchanged. Thus, a distinction can be made by looking at the background count rate. In the case of DR one expects multiexponential decay due to the disappearance of high DR-rate levels, while in the case of SEC one expects single exponential decay.

For two electron currents of $I_{el}=11$ and 47 mA, the DR rate and the background count rate were measured as a function of time. The results for the DR rates are shown in Fig. 12. One can observe that the rates for 47 mA fall by a factor of 2 during the first five seconds and another factor of 2.5 in the following 40 s. As expected, the decrease is less dramatic at $I_{el}=11$ mA, because the DR rate is proportional to the electron current. It is remarkable that the DR rate at the low electron current can even exceed that at high current between $t=50$ and $t=150$ s. Even at $t=240$ s the observed DR rates are not yet proportional to the electron current. However, we note that the DR rate at $E_{rel}=0$ eV depends strongly on the electron temperature because of the steep rise in cross section towards $E_{rel}=0$ eV [22]. It has been reported that the electron temperature may depend somewhat on the electron current [37]. Thus a strict proportionality may not be expected.

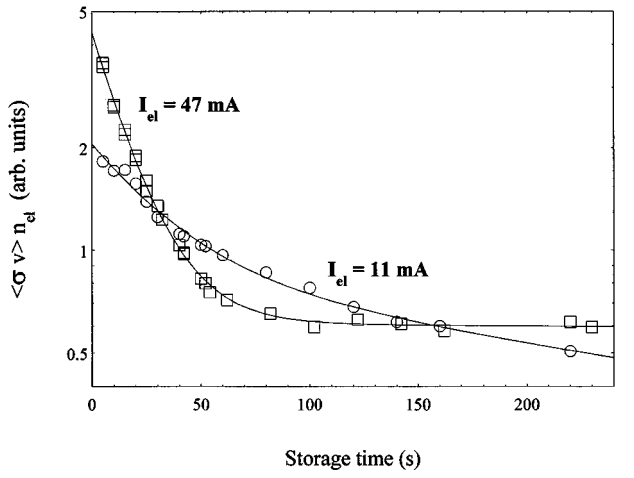

FIG. 12. Relative DR rates for H_2^+ as a function of storage time. The experiments were performed at an electron collision energy of $E_{rel}=0$ eV and for at electron currents of 11 mA (○) and 47 mA (□).

The background count rates (not shown) displayed clearly multiexponential decay behavior. The initial (at the first 10 s of storage time) decay constant, τ, of the ion beam is found to be $\tau=11$ and $\tau=23$ s (at 47 and 11 mA). The decay after 180 s gave τ values of 28 and 31 s, respectively. The lifetime of the ion beam is still affected by the cooler electrons. From the observed decay constants, the contribution of DR can be estimated to be $\tau_{DR}=300$ s at $I_{el}=47$ mA. The background signal represents the ion-beam destruction in 3.2% of the storage ring. Using $\tau_{DR}=300$ s and $\tau=28$ s for the collisional destruction, the ratio of signal to background is expected to be 2.9:1. This agrees with the intensities in Fig. 5.

The multiexponential decay of the background countrate can be explained by a loss of 15% of the beam due to DR with a decay constant, $\tau_{DR}=1.5$ s (in the case of $I_{el}=47$ mA). Hence, the DR cross section of this fraction is approximately 200 ($=300/1.5$) times higher than the DR cross section of the remaining beam. We note that the first DR rate measurement starts after about 3 s. In 3 s a fraction of 15% may be reduced by a factor of 7 to about 2%. At $t=3$ s, the DR rate is then $0.02\times200+1=5$ times larger than the DR rate at large times (squares in Fig. 12). Since the DR rate scales with the electron density, τ_{DR} is approximately 6.5 s at 11 mA. Hence, after about 35 s ($5.4\tau_{DR}$) 0.45% remains of the high DR-rate fraction. Using the DR enhancement factor of 200, this 0.45% of the ion beam is responsible for 47% of the observed DR rate. Indeed the DR rate is about a factor of 2 lower at $t=240$ s than around $t=35$ s (Fig. 12).

Above we have provided support for a ''state-specific'' DR rate of 15% of the beam to be 200 times larger than that the remaining 85%. We have not been able to reproduce the full time dependence of the DR rates quantitatively using a model that includes only two rate constants. This is not surprising as the 15% will include a number of vibrationally excited levels each with its own DR rate. This result has consequences for the comparison of different experiments, since variations in the population of such a vibrational level by 1% may change the observed DR rate by 200%. Another important conclusion is that the observed time dependencies reflect the decay of a small fraction of the ion beam. The extent of vibrational relaxation of the lower vibrational ($v^+=0-4$) levels is still unknown.

At this point it is important to consider which vibrational levels may have unusually high DR cross sections at $E_{rel}=0$. Figure 8 shows that the higher lying Q_1 states cross the H_2^+ ground-state curve near $v^+=5$, giving favorable Franck-Condon overlap at $E_{rel}=0$ eV. We note that the contribution of the $v^+\geqslant5$ levels to the ion beam is approximately 15% in the case of a (low-pressure) electron-impact source [38,39].

We want to mention one final very interesting observation. Our measurement procedure involves a determination of the count rate in the background channel (one H fragment) both with the electron cooler at $E_{\rm cool}$ ($E_{\rm rel}=0$) and at $E_{\rm meas}$ in order to correct the background signal for possible dissociative excitation. At small values of $E_{\rm rel}$ ($0.5<E_{\rm rel}<1.5$ eV) and in the first seconds of storage, the background count rate *decreased* upon changing to $E_{\rm meas}$. Apparently, a process is induced at $E_{\rm rel}=0$ eV which produces an $H+H^+$ pair in a—necessarily—endothermic reaction. We conclude that high vibrational levels ($v^+>13$) are present which have a high DR cross section and which yield one high-Rydberg state hydrogen fragment H($n>9$). These fragments are field ionized in the first bending dipole magnet after the electron cooler. Here the motional electric field is about 50 kV/cm.

IV. DISCUSSION

We have presented product state distributions from DR of H_2^+ over a large electron energy range. Dissociation into two ground-state atoms is never observed. H fragments are formed in excited states with $n>2$ if energetically possible. An indication is found for H($n>9$) fragments. At electron energies $E_{\rm rel}>12$ eV, two (correlated) H($n>1$) fragments are detected. After 20 s of storage time, $v^+>3$ ions are present in the beam. Experiments on the time dependence of the DR rate suggest that the DR cross section for high vibrational levels at $E_{\rm rel}=0$ is unusually large (more than two orders of magnitude larger than that of the lower vibrational levels). The phase-space cooling process in the electron cooler wipes out the highly excited levels via the DR process. In our opinion these observations do more than simply indicate a storage ring effect or an experimental nuisance. These observations imply that the determination of DR rates of H_2^+ in different experimental setups (single pass merged beam versus storage ring) may vary widely due to small variations of high vibrational levels in the beam. For example, single-pass crossed beam experiments using an unrelaxed ion beam will tend to produce high cross section values.

Bates [40,41] has identified many of the accepted pathways for DR. At present, nearly complete quantum-mechanical calculations show that it is often difficult to speak of one dominating DR pathway. Even in the absence of doubly excited neutral curve crossing the ionic curve (as in HeH) sizable DR cross sections are found and now theoretically reproduced. Fortunately, many observations in H_2 can be understood from the doubly excited neutral potential curves (see Fig. 8). From these curves product state distributions can not be predicted. The lowest Q_1-state, the $(2p\sigma_u)^2\ ^1\Sigma_g^+$ state, interacts with the whole manifold of $^1\Sigma_g^+$ Rydberg states. Our results show that nature tends to populate the energetically highest possible dissociation limit. More accurately stated, the $^1\Sigma_g^+$ state does not correlate exclusively with the $H(n=2)+H(n=1)$ dissociation limit. Beautiful quantitative experiments have been performed using the TSR (Test Storage Ring) in Heidelberg, where Zajfman and co-workers came to similar conclusions with HD^+ [28]. The quality of their spectra and the fact that their HD^+ beam contains only HD^+ ($v=0$) allowed them to quantify the branching over the $n=2$ to $n=4$ limits.

Dunn and co-workers [42,43] have observed fluorescence from excited D atoms resulting from DR in a crossed beam setup. They reported the production of $n=4$ and $n=2$ ($2p$). They already concluded that the production cross section of $D(2p)$ was much smaller than the total DR cross section. Mitchell and co-workers employed a single-pass merged-beams technique to study DR with very high (electron energy) resolution [13]. Using field ionization they observed a significant production (10%) of very high n ($10<n<25$) atomic Rydberg fragments at small electron energies [44,45]. These observations also pointed at the presence of highly excited vibrational levels for energy conservation. The term ''super dissociative recombination'' for the DR of high-vibrational levels of H_2^+ has been used for these levels [44,45]. Bates [46] has coined this term for unusually large DR rates in the case of potential crossings with favorable Franck-Condon overlap that involve Rydberg states converging to repulsive ionic states as in the present case of H_2^+.

An alternative way to study the ''half-collision'' dissociation process may be by using laser excitation of the $^1\Sigma_g^+$ state (or any of the higher-lying repulsive states). Indeed, using resonance enhanced multiphoton ionization studies (REMPI) in H_2, Xu *et al.* [47] and Verschuur *et al.* [48] have observed dissociation of H_2. Photoelectron spectroscopy on the H fragments was used to determine qualitatively the product state distribution. Hardly any H($n=2$) was observed, and roughly equal amounts of H($n=4$ and 5) [48]. However, the translation of these results to the dynamics during DR is not completely clear. Theoretical predictions on the half-collision problem are scarce. Zhdanov and Chibisov [49] have performed calculations in which H(n) products are formed through higher-lying doubly excited states $^{1,3}\Lambda(2p\sigma,nl\lambda)$ assuming conservation of the quantum number ''n'' during dissociation. However, the present results suggest that even the lowest doubly excited state in H_2 can give rise to H($n\geqslant 3$) fragments. Hence, no simple relation exists between the molecular configuration and the resulting atomic fragments.

The arrival of dedicated experiments to probe product states will enhance the attention for this aspect of DR. Mechanistic information on DR can also be obtained from the angular distributions of the DR fragments. At $E_{\rm rel}$ values significantly above the temperature of the cooler electrons (100 K), the relative collision velocity is parallel to the ion-beam velocity. As the dissociation is prompt [50,51], angular distributions are expected between $\sigma(\theta)=\cos^2\theta$ and $\sin^2\theta$, depending on the molecular symmetry of the states involved. Zajfmann *et al.* [28] have observed these angular distributions and concluded that the dominant channel around $E_{\rm rel}=8$ eV (in the case of HD^+) is due to a repulsive state with $^3\Sigma_u^+$ symmetry. This conclusion does not seem to be supported by quantum-mechanical calculations [21,52].

Our identification of vibrational states in an H_2^+ ion beam with ''super'' DR rates is important. In the case of D_2^+ vibrational cooling through selective destruction by rest gas collisions was invoked to be the cause of changes in the DR rates [18]. The present experiments show that the electron-ion interactions are responsible for changes in the ion-beam population. In ASTRID (The Aarhus Storage Ring, Denmark), laser photodissociation has been applied to photodissociate high-vibrational excited levels. These levels were found to be present after 60 s of storage time [53].

For heteronuclear systems (and homonuclear with two isotopes), storage times of a few seconds generally suffices for complete intramolecular cooling through radiative processes. But, in the case of homonuclear systems, such as H_2^+ and O_2^+, the development of ion sources which deliver vibrational ground-state ions only is advisable. Mitchell and co-workers have tried to optimize an ion source to produce vibrationless molecular ions [54]. A cooled hollow-cathode ion source can produce an O_2^+ ($v^+=0$) beam, as has been shown using a dissociative charge-transfer collision [55] to probe the population.

In the present experiments changes have been seen in the vibrational population due to the DR process itself at $E_{\rm rel}=0$ eV. Preliminary quantal calculations on the size of the DR cross section show a fortyfold increase of the DR cross section of the $v=5$ and 9 levels with respect to the $v=0$ levels [52], which is less than is concluded from the experiment. In these calculations only the so-called direct channel has been taken into account.

We have mentioned superelastic collisions (SEC) but have not obtained direct proof of the importance thereof. Guberman [56] on N_2 and Sarpal and Tennyson [36] on H_2 have treated this process neglecting nonadiabatic effects. The vibrational cooling time of H_2^+ can be estimated [36] using the data at 100 K (our electron resolution is 10 meV). The interaction length ($l=0.8$ m) is 1.5% of the ring circumference of $L=52$ m. The electron density is taken to be $n_e=10^7$ cm^{-3} (15 mA). The deexcitation rates from [36] for $v^+=1$ and $v^+=2$ are $a_1=8.5\times10^{-8}$ and $a_2=1.2\times10^{-7}$ cm^3/s. The cooling rate $k_{c,i}$ for vibrational level ''i'' is now given by

$$k_{c,i}=n_e\,\frac{1}{L}\,a_i\,. \tag{4}$$

This results in cooling times ($k_{c,i}^{-1}$) of 76 s and 32 s for $v^+=1$ and $v^+=2$, respectively. Superelastic vibrational cooling rates are comparable to the DR cross sections, because SEC look like DR collisions, in which the ''survival'' part failed. Therefore, SEC may play an important role for the high-vibrational levels with the high DR rates. Sarpal and Tennyson note that the deexcitation rate of the $v^+=1$ is nearly equal to the DR rate as calculated by Giusti-Suzor, Bardsley, and Derkits [57] and Takagi, Kosugi, and Dourneuf [58], whereas the deexcitation rate of the $v^+=2$ level even exceeds the DR rate by a factor of two. Using the above cooling times, full vibrational relaxation by SEC will take many minutes.

The DR rate depends also on the rotational quantum number [59]. Regarding this degree of freedom, H_2^+ differs strongly from HD^+. As the ion source is run at rather high pressure, an elevated rotational temperature of a few 100 K is expected because of ion-molecule reactions. If radiative processes in the storage ring dominate, then HD^+ is cooled to room temperature in a few seconds whereas H_2^+ remains rotationally hot. Rotational cooling through superelastic collisions with cooler electrons will have a profoundly different effect on both isotopomers. In HD^+, cooling by SEC and heating by blackbody radiation will result in an effective temperature around the temperature of the ring of 300 K. In H_2^+, heating by black-body radiation is absent and much lower rotational temperatures may be reached. Although vibrational or rotational SEC have not been demonstrated, a lot of electron-molecular ion dynamics can be learnt using state-selective ion beams.

V. CONCLUSIONS

In this paper results have been described on dissociative recombination of H_2^+ and HD^+. Product state information has been obtained on H_2^+. A propensity to create excited hydrogen fragments, even $n>9$ Rydberg atoms, at low electron collision energies, a distinct anisotropy at higher electron energies and finally two excited atoms at the highest (15 eV) collision energies have been observed. In contrast to HD^+, an H_2^+ ion beam is found to contain vibrationally excited ions. As concluded from a strongly time-dependent DR rate, higher-vibrational levels have very high DR cross sections at least two orders of magnitude higher than the low-vibrational levels. We conclude that DR experiments on H_2 and D_2 require caution in their interpretation as small variations in the ion-beam population may have drastic effects, clearly hampering comparisons between different experimental techniques.

ACKNOWLEDGMENTS

We would like to thank A. Suzor-Weiner, I. F. Schneider, M. Chibisov, B. J. A. Mitchell, X. Urbain, S. L. Guberman, and L. H. Andersen for many stimulating discussions. B. J. A. Mitchell is thanked for sharing results prior to publication. We would also like to thank the staff members of the Manne Siegbahn Laboratory for their important contributions to the experiment and Wim Barsingerhorn from AMOLF for the construction of the ''poor man's''-position sensitive detector. The work by W.J.v.d.Z. is part of the research program of the Foundation for the Fundamental Research on Matter (FOM) and was made possible by financial support from the Netherlands Organisation for the Advancement of Research (NWO).

[1] M. R. Flannery, Adv. At. Mol. Opt. Phys. **32**, 117 (1994).
[2] J. L. Fox, in *Dissociative Recombination: Theory, Experiment and Applications*, edited by B. R. Rowe, J. B. A. Mitchell, and A. Canosa (Plenum, New York, 1993), p. 219.
[3] A. Dalgarno, in *Dissociative Recombination: Theory Experiment and Applications* (Ref. [2]), p. 243.
[4] E. Roueff and G. Pineau Des Forêts, in *Dissociative Recombination: Theory, Experiment and Applications* (Ref. [2]), p. 249.
[5] D. Smith, Chem. Rev. **92**, 1473 (1992).
[6] A. Dalgarno, Adv. At. Mol. Opt. Phys. **32**, 57 (1994).
[7] J. Tennyson, Rep. Prog. Phys. **57**, 421 (1995).
[8] B. K. Sarpal, J. Tennyson, and L. A. Morgan, J. Phys. B **27**, 5943 (1994).

[9] S. L. Guberman, Phys. Rev. A **49**, R4277 (1994).
[10] S. L. Guberman, J. Chem. Phys. **78**, 1404 (1983).
[11] N. G. Adams, in *Dissociative Recombination: Theory, Experiment and Applications* (Ref. [2]), p. 99.
[12] B. R. Rowe, in *Dissociative Recombination: Theory, Experiment and Applications* (Ref. [2]), p. 113.
[13] J. B. A. Mitchell, F. B. Yousif, P. Van der Donk, and T. J. Morgan, in *Dissociative Recombination: Theory, Experiment and Applications* (Ref. [2]), p. 87.
[14] P. Van der Donk, F. B. Yousif, J. B. A. Mitchell, and A. P. Hickman, Phys. Rev. Lett. **67**, 42 (1991).
[15] T. Tanabe, I. Katayama, N. Inoue, K. Chida, Y. Arakaki, T. Watanabe, M. Yoshizawa, S. Ohtani, and K. Noda, Phys. Rev. Lett. **70**, 422 (1993).
[16] P. Forck, M. Grieser, D. Habs, A. Lampert, R. Repnow, D. Schwalm, A. Wolf, and D. P. Zajfman, Phys. Rev. Lett. **70**, 426 (1993).
[17] M. Larsson, H. Danared, J. R. Mowat, P. Sigray, G. Sundström, L. Broström, A. Filevich, A. Källberg, S. Mannervik, K. Rensfelt, and S. Datz, Phys. Rev. Lett. **70**, 430 (1993).
[18] M. Larsson, M. Carlson, H. Danared, L. Broström, S. Mannervik, and G. Sundström, J. Phys. B **27**, 1397 (1994).
[19] M. Larsson, Int. J. Mass Spectrom. Ion Proc. **149/150**, 403 (1995).
[20] H. Danared, G. Andler, L. Bagge, C. J. Herrlander, J. Hilke, J. Jeansson, A. Källberg, A. Nilsson, A. Paál, K.-G. Rensfelt, U. Rosengård, J. Starker, and M. af Ugglas, Phys. Rev. Lett. **72**, 3775 (1994).
[21] C. Strömholm, I. F. Schneider, G. Sundström, L. Carata, H. Danared, S. Datz, O. Dulieu, A. Källberg, M. Af Ugglas, X. Urbain, V. Zengin, A. Suzor-Weiner, and M. Larsson, Phys. Rev. A **52**, R4230 (1995).
[22] J. R. Mowat, H. Danared, G. Sundström, M. Carlson, L. H. Andersen, L. Vejby-Christensen, M. af Ugglas, and M. Larsson, Phys. Rev. Lett. **74**, 50 (1995).
[23] G. Sundström, S. Datz, J. R. Mowat, S. Mannervik, L. Broström, M. Carlson, H. Danared, and M. Larsson, Phys. Rev. A **50**, R2806 (1994).
[24] G. Sundström, J. R. Mowat, H. Danared, S. Datz, L. Broström, A. Filevich, A. Källberg, S. Mannervik, K.-G. Rensfelt, P. Sigray, M. af Ugglas, and M. Larsson, Science **263**, 785 (1994).
[25] S. Datz, M. Larsson, C. Strömholm, G. Sundström, V. Zengin, H. Danared, A. Källberg, and M. af Ugglas, Phys. Rev. A **52**, 2901 (1995).
[26] S. Datz, G. Sundström, Ch. Biedermann, L. Broström, H. Danared, S. Mannervik, J. R. Mowat, and M. Larsson, Phys. Rev. Lett. **74**, 896 (1995).
[27] T. Tanabe, I. Katayama, N. Inoue, K. Chida, Y. Arakaki, T. Watanabe, M. Yoshizawa, M. Saito, Y. Haruyama, K. Hosono, T. Honma, K. Noda, S. Ohtani, and H. Takagi, Phys. Rev. A **49**, R1531 (1994).
[28] D. Zajfman, Z. Amitay, C. Broude, P. Forck, B. Seidel, M. Grieser, D. Habs, D. Schwalm, and A. Wolf, Phys. Rev. Lett. **75**, 814 (1995).
[29] W. J. van der Zande, V. Zengin, C. Strömholm, G. Sundström, and M. Larsson, in *Dissociative Recombination: Theory, Experiment and Applications*, edited by D. Zajfman, J. B. A. Mitchell, D. Habs, and B. R. Rowe (World Scientific, Singapore, 1996), p. 135.
[30] K. Abrahamsson, G. Andler, L. Bagge, P. Carlé, H. Danared, S. Egnell, K. Ehrnstén, M. Engström, C. J. Herrlander, J. Hilke, J. Jeansson, A. Källberg, S. Leontein, L. Liljeby, A. Nilsson, A. Paál, K. G. Rensfelt, U. Rosengård, A. Simonsson, A. Soltan, J. Starker, M. af Ugglas, and A. Filevich, Nucl. Instrum. Methods Phys. Res. B **79**, 269 (1993).
[31] M. Larsson and C. Strömholm, in *Dissociative Recombination: Theory, Experiment and Applications* (Ref. [29]),p. 74.
[32] G. Sundström, Ph.D. Thesis, Royal Institute of Technology Stockholm, 1994.
[33] J. R. Mowat, in *Dissociative Recombination: Theory, Experiment and Applications* (Ref. [29]), p. 226.
[34] T. E. Sharp, At. Data **2**, 119 (1971).
[35] Z. Amitay, D. Zajfman, and P. Forck, Phys. Rev. A **50**, 2304 (1994).
[36] B. K. Sarpal and J. Tennyson, Mon. Not. R. Astron. Soc. **263**, 909 (1993).
[37] H. Gao, S. Asp, C. Biedermann, D. R. DeWitt, R. Schuch, W. Zong, and H. Danared, Hyperfine Interact. **99**, 301 (1996).
[38] F. Von Busch and G. H. Dunn, Phys. Rev. A **5**, 1726 (1972).
[39] D. Villarejo, J. Chem. Phys. **49**, 2523 (1968).
[40] D. R. Bates, Phys. Rev. **78**, 492 (1950).
[41] D. R. Bates, Adv. At. Mol. Opt. Phys. **34**, 427 (1994).
[42] R. A. Phaneuf, D. H. Crandall, and G. H. Dunn, Phys. Rev. A **11**, 528 (1975).
[43] M. Vogler and G. H. Dunn, Phys. Rev. A **11**, 1983 (1975).
[44] J. B. A. Mitchell, F. B. Yousif, P. J. T. Van der Donk, J. Morgan, and M. I. Chibisov, Int. J. Mass Spec. Ion Proc. **149/150**, 153 (1995).
[45] M. I. Chibisov, F. B. Yousif, P. J. T. Van der Donk, J. B. A. Mitchell, and T. J. Morgan, in *Dissociative Recombination: Theory, Experiment and Applications* (Ref. [29]), p. 100; M. I. Chibisov, J. B. A. Mitchell, P. J. T. Van der Donk, F. B. Yousif, and T. J. Morgan (unpublished).
[46] D. R. Bates, J. Phys. B **24**, 703 (1991).
[47] E. Y. Xu, T. Tsuboi, R. Kachru, and H. Helm, Phys. Rev. A **36**, 5645 (1987).
[48] J. W. J. Verschuur, L. D. Noordam, J. H. M. Bonnie, and H. B. van Linden, Chem. Phys. Lett. **146**, 283 (1988).
[49] V. P. Zhdanov and M. I. Chibisov, Zh. Eksp. Teor. Fiz. **74**, 75 (1978) [Sov. Phys. JETP **74**, 38 (1978)].
[50] G. H. Dunn, Phys. Rev. Lett. **8**, 62 (1962).
[51] R. N. Zare, J. Chem. Phys. **46**, 204 (1966).
[52] I. F. Schneider and A. Suzor-Weiner (private communication).
[53] H. T. Schmidt, L. Vejby-Christensen, H. B. Pedersen, D. Kella, N. Bjerre, and L. H. Andersen, J. Phys. B **29**, 2485 (1996).
[54] H. Hus, F. Yousif, C. Noren, A. Sen, and J. B. A. Mitchell, Phys. Rev. Lett. **11**, 1006 (1988).
[55] W. J. van der Zande, J. R. Peterson, and P. C. Cosby (unpublished).
[56] S. Guberman, in *Dissociative Recombination: Theory, Experiment and Applications* (Ref. [2]), p. 47.
[57] A. Guisti-Suzor, J. N. Bardsley, and C. Derkits, Phys. Rev. A **28**, 682 (1983).
[58] H. Takagi, N. Kosugi, and M. Dourneuf, J. Phys. B **24**, 711 (1991).
[59] H. Takagi, J. Phys. B **26**, 4815 (1993).